Engineering DNA Crystals towards Studying DNA-Guest Molecule Interactions

Cuizheng Zhang^{1#}, Jiemin Zhao^{1,2#}, Brandon Lu³, Nadrian C. Seeman^{3†}, Ruojie Sha³, Nicholas Noinaj⁴, Chengde Mao^{1*}

²Institute of Clinical Pharmacology, Key Laboratory of Anti-Inflammatory and Immune Medicine, Ministry of Education, Anhui Collaborative Innovation Center of Anti-Inflammatory and Immune Medicine, Anhui Medical University, Hefei, China, 230032

Abstract. Sequence-selective recognition of DNA duplex is important for a wide range of applications including regulating gene expression, drug development, and genome editing. Many small molecules can bind DNA duplexes with sequence selectivity. It remains as a challenge how to reliably and conveniently obtain the detailed structural information of DNA-molecule interaction because such information is critically needed for understanding the underline rules of DNA-molecule interactions. Only if understanding those rules, we could design molecules to preferably recognize DNA duplexes with sequence preference and intervene related biological processes, such as disease treatment. Here, we have demonstrated that DNA crystal engineering is a potential solution. A molecule-binding DNA sequence is engineered to self-assemble into highly ordered DNA crystals. X-ray crystallography study of the molecule-DNA co-crystals reveals the structural details on how the molecule interacts with the DNA duplex. In this approach, the DNA will serve two functions: (1) being part of the molecule to be studied and (2) forming the crystal lattice. It is conceivable that this method will be a general method for studying drug/peptide-DNA interactions. The resulting DNA crystals may also find use as separation matrices, as hosts for catalysts, and as media for material storage.

¹Department of Chemistry, Purdue University, West Lafayette, IN 47907, USA

³Department of Chemistry, New York University, New York, NY 10003, USA

⁴Department of Biological Sciences, Markey Center for Structural Biology, and the Purdue Institute of Inflammation, Immunology and Infectious Disease, Purdue University, West Lafayette, IN 47907, USA

^{*}These authors contribute equally

^{*}Corresponding author: mao@purdue.edu

INTRODUCTION

Sequence-selective recognition of DNA duplex is important for a wide range of applications including regulating gene expression, ¹⁻³ drug development, ⁴⁻⁶ and genome editing. ⁷⁻¹⁰ Many small molecules can bind DNA duplexes with sequence selectivity. Such binding have been extensively studied. ¹¹⁻¹⁸ However, their structural study relies most on unpredictable crystallization (for X-ray crystallography) ¹¹⁻¹⁴ or needs complicated data interpretation study (for NMR study). ^{15, 16} A reliable and convenient approach for structural study is highly desirable as structural information would help designing molecules to bind to DNA duplexes with both highly affinities and selectivities. ^{17, 18} Here, we have reported such an approach based on engineering DNA crystals. In this approach, the DNA serves two functions: (1) as part of the molecule to be studied and (2) forming the crystal lattice. This concept is demonstrated by the X-ray crystallography study of DNA-Hoechst 33342 binding.

The key of this approach is engineering high-resolution of DNA crystals. DNA as a programmable biomolecule provides a general and powerful tool for crystal engineering and nanoconstructions. ¹⁹⁻³⁰ Though a series of engineered 3D DNA crystals have been reported, ^{25, 31-41} they exhibit only modest quality of 3D order with modest X-ray diffraction resolutions. Such modest resolutions limit the applications of DNA crystals such as organizing guest molecules into hybrid crystals for structural determination by X-ray diffraction. ^{19, 42} An urgent and critical problem is how we can engineer highly ordered DNA crystals. Herein, we have developed a class of DNA motifs that can self-assemble into predesigned, well-ordered, 3D crystals that diffract to high resolutions. The crystals have either 3- or 4-fold screw axes programmed through the fine tuning of the molecular designs. Each DNA motif consists of only two short DNA strands, either identical or different. The precise molecular arrangement in the crystals has been confirmed by X-ray diffraction to a resolution of up to 2.2 Å. As a result, these DNA crystals can precisely order guest molecules in 3D space, for example, to use-the engineered DNA crystals to study DNA-guest molecule interactions.

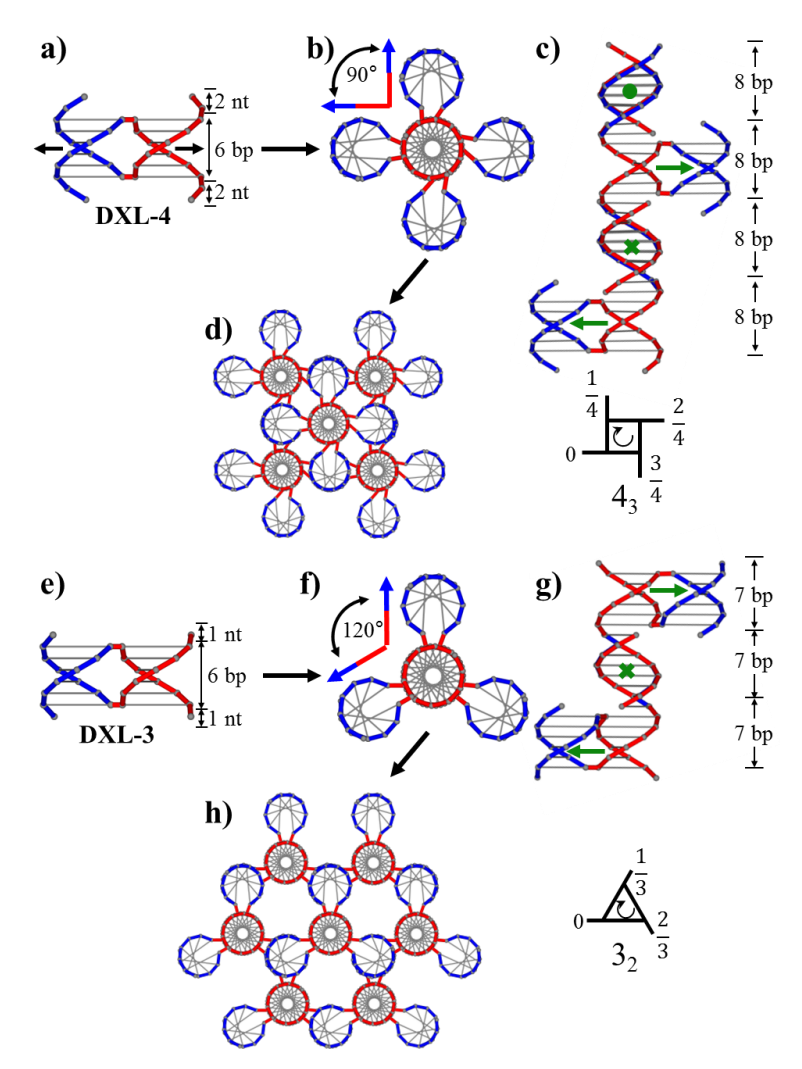


Figure 1. Designing self-assembly of DNA 3D crystals in the P4₃22 (a-d) or P3₂ (e-h) space groups. (a) Scheme of a double-crossover-like motif, DXL-4, which is a two-stranded complex. A pair of horizontal arrows indicates a 2-fold rotational axis (in term of DNA backbones). The pair of red sticky ends is complementary to each other; the same to the pair of blue sticky ends. Four motifs associated along one duplex via sticky-end cohesion viewed (b) along and (c) perpendicular to the duplex. A 4₃ screw axis exists along each pseudo-continuous duplex. (d) Further sticky-end cohesion leads to DNA crystals (viewed along duplexes) in the P4₃22 space group. (e) Scheme of motif DXL-3 for crystals with P3₂ symmetry group. Three motifs associated along one duplex via sticky-end cohesion viewed (f) along and (g) perpendicular to the duplexes. A 3₂ screw axis exists along each pseudo-continuous duplex. (h) Further sticky-end cohesion leads to DNA crystals (viewed along duplexes) in the P3₂ space group.

The crystal assembly is based on a two-stranded, double crossover-like (DXL) motif (Figure 1). Each DXL motif consists of two, either identical or different, single-stranded DNAs (ssDNAs). The motif is organized into two, half-turn (6-base pair, bp)-long, helical domains and each of them is flanked by a pair of short, complementary sticky ends. The motif has an out-of-plane, two-fold rotational axis in terms of the DNA backbone. Depending on the length of sticky

ends, sticky end-cohesion will allow the DXL motifs to assemble into two families of crystals with two different DNA arrangements. They are in P4₃22 and P3₂ space groups and contain 4- or 3-fold screw axes, respectively; correspondingly, the motifs are named DXL-4 or DXL-3 according to the main screw axes, respectively. All DNA duplexes are orientated in the same direction in each crystal.

RESULTS AND DISCUSSION

We first investigate crystals with P4₃22 space group (Figs. 1a-1d). These crystals are assembled from a symmetric motif, DXL-4, whose sticky ends are two nucleotides (nts) long and self-complementary. DXL-4 is a homodimeric complex of a 16 nt-long ssDNA (Fig. 1a), which is composed of four sequential, palindromic sequences with length of 2, 6, 6, and 2 nts, respectively. When two DXL-4 motifs associate through sticky-end cohesion at either the 5'- or 3'-end, one motif, relative to the other, translates along the interacting duplex by 8 base pairs (bps) and rotates right-handedly around the interacting duplex by $360^{\circ} \times 8/10.5 = 274^{\circ} \sim 270^{\circ}$ (assuming 10.5 bps per turn). Every four motifs will complete three full turns. In other words, the repeating distance along the duplex is four DXL-4 motifs, $4\times8=32$ bps. Thus, there is a 43 screw axis along the duplex. When viewing along the interacting duplex, the other helical domains of the motifs are arranged around the interacting duplex and separated away from each other by ~ 270° right-handedly (Fig. 1b and 1c). The same will happen to all other duplexes. In the final crystal, all DNA duplexes are in parallel to each other in a tetragonal fashion (Fig. 1d). From this model, we can calculate the unit cell parameters based on the parameters of an ideal B-type DNA duplex (assuming the duplex diameter is 20 Å; the rise is 3.3 Å per bp; and there is no space between adjacent duplexes), a = b = 28.3 Å and c = 105.6 Å (Fig. S1a).

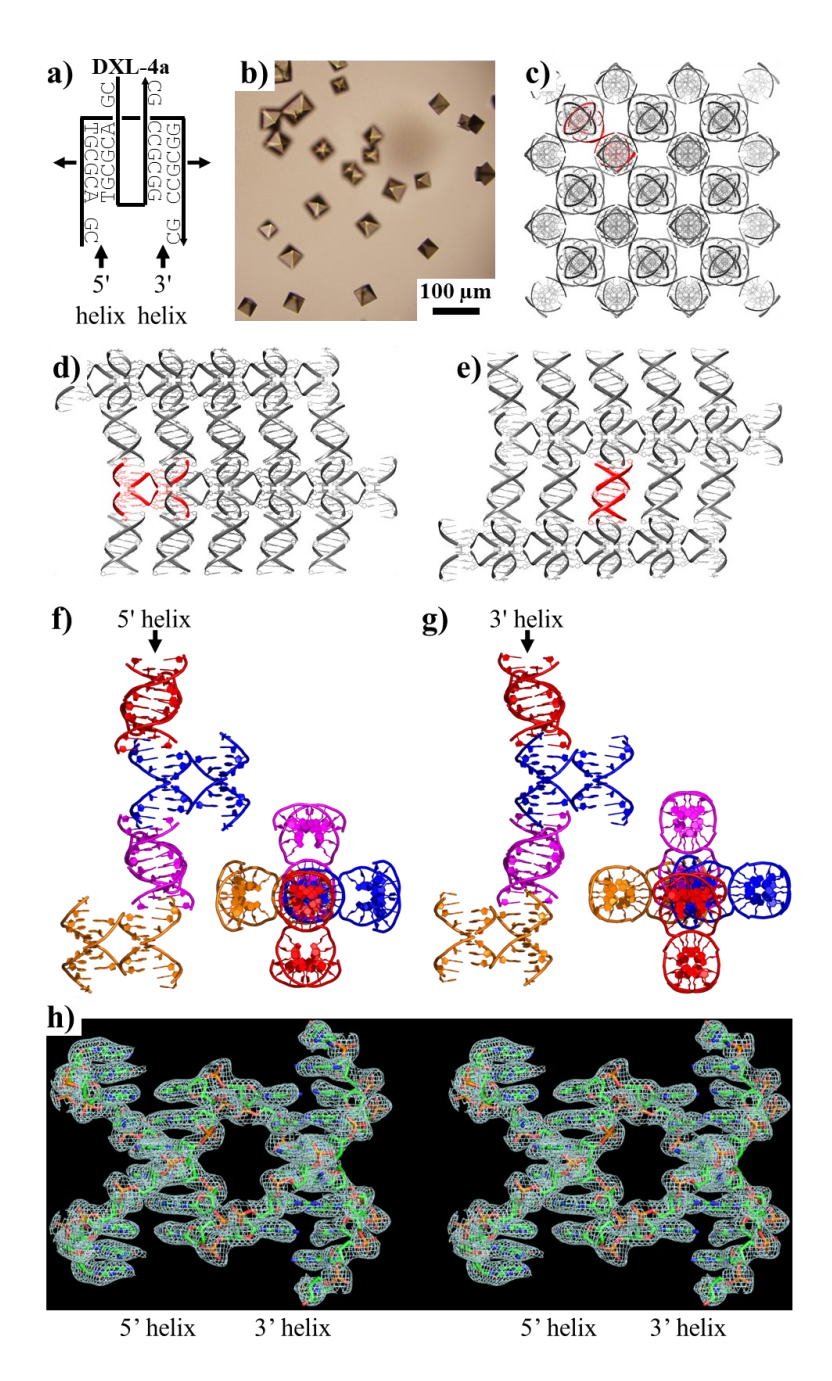


Figure 2. Experimental validation of the P4₃22 crystal assembled from motif DXL-4a. (a) The secondary structure of the symmetric motif DXL-4a. A pair of vertical and horizontal arrows indicate the 5' ends and the 2-fold rotational axis of the motif, respectively. (b) An optical image of the assembled, tetragonal bipyramid crystals. (c-e) Three orthogonal views (along [0,0,1], [1,1,0] and [1,-1,0]) of the DNA arrangement in the crystals. One DXL-4a motif is highlighted in red. (f) and (g) Four (colored differently) associated DXL-4a motifs along the 5' and 3' helixes, respectively. Each is presented with a pair of views along and perpendicular to the associating helix. (h) A pair of stereo images of the DXL-4a motif with 2Fo-Fc electron density map contoured at 1.0σ and 2.2 Å resolution.

Motif	Space Group	Resolution (Å)	Unit Cell					
			a (Å)	b (Å)	c (Å)	α	β	γ
DXL-4 Designed	P4 ₃ 22		28.3	28.3	105.6	90°	90°	90°
DXL-4a PDB: 8EPG	P4 ₃ 22	2.15	35.3	35.3	104.4	90°	90°	90°
DXL-4b PDB: 8EP8	P4 ₃ 22	2.45	33.0	33.0	104.3	90°	90°	90°
DXL-4c PDB: 8EPE	P4 ₃ 22	2.45	34.9	34.9	105.0	90°	90°	90°
DXL-4d PDB: 8EPD	P4 ₃ 22	2.42	34.2	34.2	104.3	90°	90°	90°
DXL-4e PDB: 8EPI	P4 ₃ 22	2.56	36.4	36.4	104.4	90°	90°	90°
DXL-4f PDB: 8EPF	P4 ₃	2.61	33.6	33.6	106.0	90°	90°	90°
DXL-4g PDB: 8F40	P4 ₃ 22	2.45	36.8	36.8	103.3	90°	90°	90°
DXL-4g/ Hoechst 33342 PDB: 8F42	P4 ₃	2.55	35.4	35.4	103.3	90°	90°	90°
DXL-3 Designed	P3 ₂		34.6	34.6	69.3	90°	90°	120°
DXL-3 Observed PDB: 8EPB	P3 ₂	2.61	38.0	38.0	69.6	90°	90°	120°

Table 1. Comparison of crystal parameters from design and experiments for all crystal designs in this work.

The ssDNAs first homodimerize into the DXL-4a motif, and then further assemble into crystals in a hanging drop setting (Figure 2). The crystals appeared as tetragonal bipyramids, reflecting the designed P4322 space group (Fig. 2b). The crystals were highly ordered and diffracted well under X-ray. Based on the diffraction data, the crystal structure has been solved by molecular replacement to a resolution of 2.2 Å. The solved crystal structure fully validated our design and also revealed some unexpected, structural details. There is a good match between the crystal parameters between the designed model and the experimental characterized crystals (Table 1). In the DNA crystals, all DNA duplexes are parallel to each other in a tetragonal arrangement (Fig. 2c-e). Any two interacting DNA motifs associate with each other along either 5' or 3' helixes, but not both. One motif, relative to the other, not only translates along the interacting duplex, but also rotates right-handedly around the interacting duplex by 270°. Overall, the duplexes associate with each other to form pseudo-continuous, parallel helixes to run through the entire crystals. Any pseudo-continuous helix is composed of only 5' or only 3' helixes of the motifs. 5' and 3' helixes are in an alternating arrangement in the crystals. A phenomenon unexpected from the design is that 5' helixes and 3' helixes behave quite differently (Fig. 2f and 2g). While the 5' helixes are fairly straight (Fig. 2f), the 3' helixes swirl around the helical axes due to significant duplex bending at the sticky-end regions (Fig. 2g). Such swirling effect explains the substantial difference of the unit cell dimensions in a and b between what designed

and what observed (Table 1). The structural details of the observed individual DXL-4a motif are shown in Fig. 2h as a pair of stereo images. The structural model and the observed electron density map closely match with each other. When a higher contour level is applied to the electron density map, the remaining, isolated, electron densities locate to the phosphate locations, which have the highest densities as phosphorus is the heaviest atom in the DNA molecule (Fig. S2), confirming that the structural model is correct. As such, the model captures all the main features from our design. It contains two, vertically aligned, half-turn, right-handed, helical domains and each domain is flanked by two 2-nt-long ssDNA overhangs. Note that the surface of each face of the motif has very different tomography (Fig. S3). Judging from the B-factors, the 5' domain of the motif is quite rigid, but the 3' domain contains certain flexibility (Fig. S4). Though the DXL-4a motif consists of two half-turn right-handed helical domains, its backbones globally form a one-turn, left-handed, double helix as we proposed before. In the global left-handed duplex, all base pair planes are parallel to the helical axis.⁴³

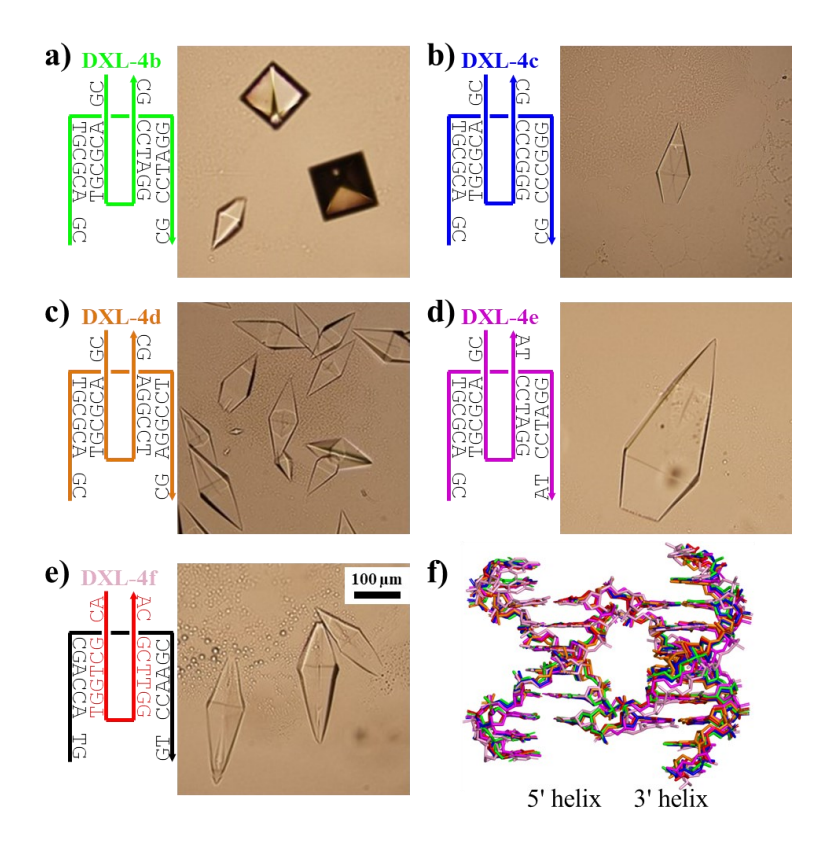


Figure 3. P4₃22 crystal design is robust to sequence variation. (a) symmetric DXL-4b, (b) symmetric DXL-4c, (c) symmetric DXL-4d, (d) symmetric DXL-4e, (e) asymmetric DXL-4f. These designs have different base compositions and sequences. Each panel contains (left) the motif secondary structure and (right) an optical image of the corresponding crystals. (f) Superimposition of five DXL variations with DXL-4a (red). The color codes are the same as the motif names.

The above motif design has a strict requirement for the DNA secondary structure (e.g. the length and sequence complementarity of each domain), but not the exact sequence. To demonstrate the sequence versatility, we have designed another five different versions of DNA DXL-4 variations and test their capability to assemble into P4₃22 crystals. (Figure 3). Those motifs are either symmetric, homo-dimeric complexes (Fig. 3a-3d) or an asymmetric hetero-dimeric complex (Fig. 3e). These variations differ from each other in GC contents, junction sequences, or sticky-end sequences. They all assembled into high quality crystals in the P4₃22 (for symmetric motifs) or P4₃ (for the asymmetric motif) space groups. All crystals are nearly identical to one another in terms of crystal morphology, DNA arrangement, and unit cell dimensions (Table 1). When superimposing the solved crystal structure of all DXL-4 motifs, the root-mean-square deviation (RMSD) is very low (in the range of 0.31 – 0.57) (Figs. 3f and S5), indicating that the design is robust in terms of sequence variations.

The overall design principle is robust. We have further applied the design principle to design DNA crystals in the P3₂ space group (Fig. 1e-1h). These crystals are assembled from an asymmetric DNA motif, DXL-3. The DXL-3 motif (Figs. 1e and 4a) is almost identical to the asymmetric DXL-4f (Figs. 1a and 3e) except the DXL-3 has 1-nt-long sticky ends but the DXL-4f has 2-nt-long sticky ends. The two sticky ends on the two 5' ends of the motif are complementary to each other; the same to those on the 3' ends. The DXL-3 motif is a complex of two different, 14-nt-long ssDNAs. When two DXL-3 motifs associate through sticky-end cohesion, one motif, relative to the other, translates along the interacting duplex by 7 bps and rotates right-handedly around the interacting duplex by $360^{\circ} \times 7/10.5 = 240^{\circ}$ (Figs. 1f and 1g). Every three motifs will complete two, right-handed turns. Thus, there is a 3₂ screw axis along the interacting duplex. When viewing along this duplex, the other helical domains of the motifs are arranged around the interacting duplex and separated away from each other by ~ 240° right-handedly (Figs. 1f and 1g). The same will happen to all other duplexes. In the final crystal, all DNA duplexes are parallel to each other in a trigonal fashion (Fig. 1h). From this model, we can calculate the unit cell parameters as: a = b = 34.6 Å and c = 69.3 Å (Fig. S1b).

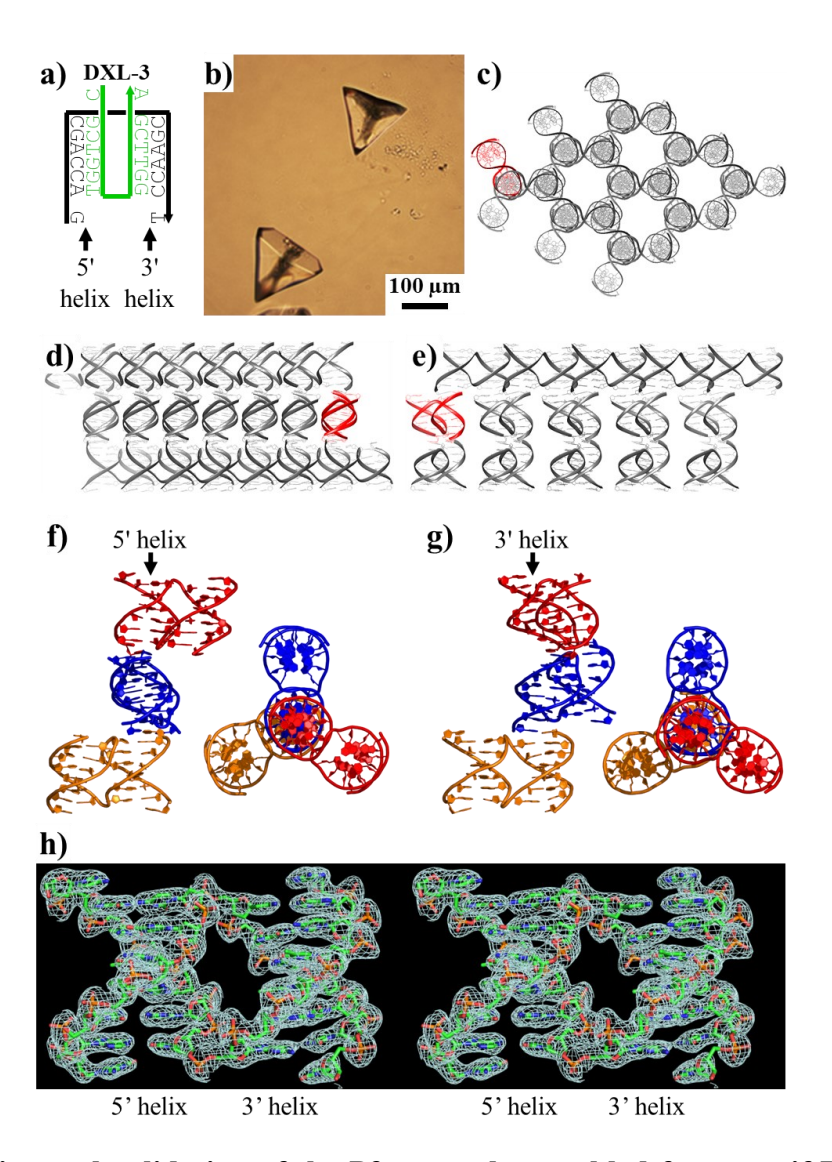


Figure 4. Experimental validation of the P32 crystal assembled from motif DXL-3. (a) The secondary structure of the asymmetric motif DXL-3. (b) An optical image of the assembled crystals. (c-e) Three orthogonal views (along [0,0,1], [1,0,0] and [0,1,0]) of the DNA arrangement in the crystals. One DXL-3 motif is highlighted in red. (f) and (g) Three (colored differently) associated DXL-3 motifs along the 5' and 3' helixes, respectively. Each is presented with a pair of views along and perpendicular to the associating helix. (h) A pair of stereo images of the DXL-3 motif with 2Fo-Fc electron density map contoured at 1.0σ and 2.6 Å resolution.

When mixing the two component strands of DXL-3 together in a hanging drop setup, the DNA readily assembled into high quality crystals with triangular shapes (Figure 4), consistent with the intrinsic P32 symmetry. The crystals were highly ordered and diffracted well, allowing the crystal to be solved at a resolution of 2.6 Å by molecular replacement. Unlike the close-packing in the P4322 crystals, the P32 crystals appear to be quite porous. DNA duplexes run in the same direction arranged in honeycomb lattices. Continuous, uniform channels (about 22 Å in diameter) run parallel to the DNA duplexes through the crystals (Fig. 4c). Figures 4f and 4g

show three DXL-3 motifs associated with each other along 5' and 3' helixes, respectively. Each has one pair of views along and perpendicular to the DNA duplexes. The unit cell parameters observed in the crystal (Table 1) matches those predicted from the design. The only significant difference is the values for a and b resulting from the swirling of the 3' helixes (Fig. 4g). When increasing the contour level of the electron density map, the remaining electron densities locate on the phosphorus atoms, the heaviest atoms in DNA (Fig. S6); further confirming the structural model. The motif structure is rigid in both 5' and 3' helixes shown by the B-factor analysis (Fig. S7).

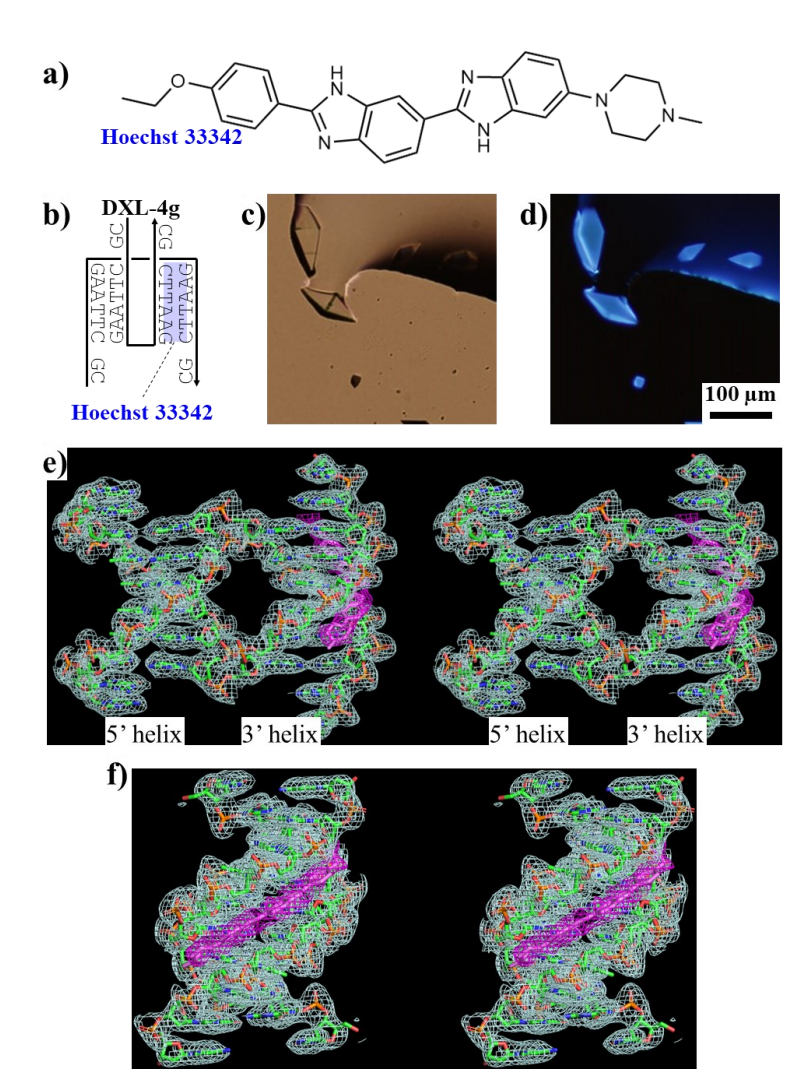


Figure 5. Organization of Hoechst 33342 by engineered a P43 DNA crystal. (a) Hoechst 33342 structure. (b) Motif DXL-4g/Hoechst complex. (c) Bright field and (d) fluorescence images of DNA-Hoechst 33342 complex crystals. (e) and (f) Two pairs of stereo images of the solved crystal structure of DXL-4g/Hoechst 33342 complex viewed from two different orientations with 2Fo-Fc electron density map contoured at 1.0σ for DXL-4g and 0.5σ for Hoechst 33342 and 2.55 Å resolution. Hoechst 33342 in purple.

To demonstrate that we can use the engineered DNA crystals to study DNA-guest molecule interaction, we have chosen Hoechst 33342 as the model guest molecule. DNA-Hoechst 33342 binding have been crystallographically studied before;¹¹ thus the structural information could be used to validate our proposed method. A longstanding promise of DNA crystal engineering, since 1982, is to use DNA crystals to precisely organize guest molecules in the 3D space. 19 Such a study has not been possible for at least one decade because of the modest resolution of previously designed DNA crystals. The high resolution achieved in this study enables such applications. We have engineered a DNA crystal to study the interaction between DNA and Hoechst 33342 (Figure 5). Hoechst is a blue-color fluorescence molecule and can bind to the minor groove of DNA duplex, preferably at A/T-rich sequences (5'-GAATTC-3'). We have designed a P4₃22 crystal-forming, symmetric motif, DXL-4g because of the robustness of sequence variation. It contains one Hoechst 33342 binding site at its 3' duplex. DXL-4g alone readily assembled into P4322 crystals in the same way as other DXL-4 motifs (Fig. S8). In the presence of Hoechst 33342, the DXL-4g assembled into crystals with the same morphology, but with blue fluorescence because of the emission of Hoechst 33342 under UV light (Figs. 5c and 5d), indicating that Hoechst 33342 was incorporated into the DNA crystals. The crystals diffracted well and the structure had been solved to a resolution of 2.55 Å. The Hoechst 33342 molecule could be unambiguously modeled into the electron density map. The molecule bound to the minor groove of the 3' helix at the sequence of 5'-GAATTC-3' as the predicted. The binding interaction between the DNA duplex and Hoechst 33342 in this study was almost the same as the previously reported crystal structure of DNA duplex-Hoechst 33342 (PDB ID: 129D) which could be seen from the structure superposition (Fig. S9). 11 Furthermore, DXL-4g structure didn't change significantly with or without Hoechst 33342 (Fig. S10) but had a significant difference in the Fo-Fc map (Fig. S11).

CONCLUSION

In summary, this study has several important advancements. (1) we have developed a design principle to engineer precisely ordered, symmetry-tunable, DNA crystals that diffract to 2.2 Å. Compared with previously reported systems of engineered DNA crystals, the current building motif is small with only 1 or 2, unique, 14- or 16-nt-long, ssDNAs. Particularly, the length of the motif along the helical axis is short (7 or 8 bps long). The motif has an overall isotropic geometry (2×4×2.5 nm). We believe that these factors together contribute to the high crystal orders, which enables high resolution. (2) We have demonstrated that the engineered crystals could be used to study the structural details of DNA-guest molecule interactions. Here the DNA forms the crystal lattices and is part of the molecule to-be-studied. As the motifs here could accommodate different DNA sequences and most drugs recognize only up to 6 base pairs, 11-15, 17, 18 this system could allow study of a wide range of DNA-drug interactions. (3) In the crystals, the interhelical angles of the DNA junctions are $\sim 0^{\circ}$ as in most of the DNA nanostructures^{21-24, 26-30} (in contrast to 40-60° in previously reported crystal structures of DNA 4-arm junctions^{25, 31-37, 39-41, 44}). The obtained, detailed, structure of the DNA junctions in this configuration would be highly valuable for designing fine DNA nanostructures at the Å-level. (4) It is conceivable that the engineered DNA crystals would provide a platform to precisely organize guest molecules. In the P32 crystals, the 2-nm-wide, continuous channels could accommodate up-to-2-nm guest objects, including most organic compounds, peptides,

oligosaccharides, small nucleic acids (aptamers, ribozymes, and DNAzymes), and small proteins. The engineered DNA crystals may also be explored for other applications such as for catalysis, ⁴⁵⁻⁴⁷ separation, ⁴⁸⁻⁵¹ and information ⁵²⁻⁵⁴ and matter storage. ^{55, 56}

Supporting Information

Materials and detailed experimental methods of crystallization and crystallography; and figures for additional crystallographic analysis.

Corresponding Author

Chengde Mao – Department of Chemistry, Purdue University, West Lafayette, Indiana 47907, United States; orcid.org/0000-0001-7516-8666; Email: mao@purdue.edu

Authors

Cuizheng Zhang – Department of Chemistry, Purdue University, West Lafayette, Indiana 47907, United States

Jiemin Zhao – Institute of Clinical Pharmacology, Anhui Medical University, Hefei, China; Department of Chemistry, Purdue University, West Lafayette, Indiana 47907, United States

Brandon Lu – Department of Chemistry, New York University, New York, New York 10003, United States

Ruojie Sha – Department of Chemistry, New York University, New York, New York 10003, United States

Nadrian C. Seeman – Department of Chemistry, New York University, New York, New York 10003, United States; orcid.org/0000-0002-9680-4649

Nicholas Noinaj – Department of Biological Sciences, Markey Center for Structural Biology, and the Purdue Institute of Inflammation, Immunology and Infectious Disease, Purdue University, West Lafayette, Indiana 47907, United States

Author Contributions

[#]C. Z. and J. Z. contributed equally to this work.

Notes

The authors declare no competing financial interest.

Data availability

Crystallography data are available from the Protein Data Bank (https://www.rcsb.org/) with access codes 8EPG, 8EPB, 8EPB, 8EPB, 8EPB, 8EPB, 8F40 and 8F42.

Acknowledgement

[†]In memory of Prof. Nadrian C. Seeman. He passed away in November 16, 2021 during this study.

This work was financially supported by NSF (CCF-2107393 and CCMI-2025187 to C.M.), NIH/NIGMS (1R01GM127884 and 1R01GM127896 to N.N.) and the Youth Fund of Anhui Medical University (2022xkj009 to J.Z.).

References

- 1. Francois Jacob and Jacques Monod. Genetic Regulatory Mechanisms in the Synthesis of Proteins. *J. Mol. Biol.* **3**, 318-356 (1961).
- 2. Babak Alipanahi, Andrew Delong, Matthew T Weirauch and Brendan J Frey. Predicting the Sequence Specificities of DNA- and RNA-Binding Proteins by Deep Learning. *Nat. Biotechnol.* **33**, 831-838 (2015).
- 3. Eeshit Dhaval Vaishnav, Carl G. de Boer, Jennifer Molinet, Moran Yassour, Lin Fan, Xian Adiconis, Dawn A. Thompson, Joshua Z. Levin, Francisco A. Cubillos and Aviv Regev. The Evolution, Evolvability and Engineering of Gene Regulatory DNA. *Nature* **603**, 455-463 (2022).
- 4. Patricia M. Takahara, Amy C. Rosenzweig, Christin A. Frederick and Stephen J. Lippard. Crystal Structure of Double-Stranded DNA Containing the Major Adduct of the Anticancer Drug Cisplatin. *Nature* **377**, 649-652 (1995).
- 5. Qi Gao, Loren Dean Willams, Martin Egli, Dov Rabinovich, Shun-Le Chen, Gray J. Quigley and Alexander Rich. Drug-induced DNA repair: X-ray Structure of a DNA-Ditercalinium Complex. *Proc. Natl. Acad. Sci. U. S. A.* 88, 2422-2426 (1991).
- 6. Yi Gui Gao, Yen Chywan Liaw, Howard Robinson and Andrew H. J. Wang. Binding of the Antitumor Drug Nogalamycin and its Derivative to DNA: Structural Comparison. *Biochemistry* **29**, 10307-10316 (1990).
- 7. Aron M. Geurts, Gregory J. Cost, Yevgeniy Freyvert, Bryan Zeitler, Jeffrey C. Miller, Vivian M. Choi, Shirin S. Jenkins, Adam Wood, Xiaoxia Cui, Xiangdong Meng, Anna Vincent, Stephen Lam, Mieczyslaw Michalkiewicz, Rebecca Schilling, Jamie Foeckler, Shawn Kalloway, Hartmut Weiler, Séverine Ménoret, Ignacio Anegon, Gregory D. Davis, Lei Zhang, Edward J. Rebar, Philip D. Gregory, Fyodor D. Urnov, Howard J. Jacob and Roland Buelow. Knockout Rats via Embryo Microinjection of Zinc-Finger Nucleases. *Science* 325, 433 (2009).
- 8. J. Keith Joung and Jeffry D. Sander. TALENs: a widely applicable technology for targeted genome editing. *Nat. Rev. Mol. Cell Biol.* **14**, 49–55 (2013).
- 9. Jennifer A. Doudna and Emmanuelle Charpentier. The New Frontier of Genome Engineering with CRISPR-Cas9. *Science* **346**, 1258096 (2014).
- 10. Patrick D.Hsu, Eric S.Lander and Feng Zhang. Development and applications of CRISPR-Cas9 for genome engineering. *Cell* **157**, 1262-1278 (2014).

- 11. M. Sriram, Gijs A.van der Marel, Harlof L.P.F. Roelen, Jacques H.van Boom and Andrew H.-J. Wang. Conformation of B-DNA Containing O6-ethyl-G-C Base Pairs Stabilized by Minor Groove Binding Drugs: Molecular Structure of d(CGC[e6G]AATTCGCG Complexed with Hoechst 33258 or Hoechst 33342. *EMBO J.* 11, 225-232 (1992).
- 12. Lydia Tabernero, Nuria Verdaguer, Miquel Coll, Ignasi Fita, Gijs A. van der Marel, Jacques H. van Boom, Alexander Rich and Joan Aymami. Molecular Structure of the A-Tract DNA Dodecamer d(CGCAAATTTGCG) Complexed with the Minor Groove Binding Drug Netropsin. *Biochemistry* **32**, 8403-8410 (1993).
- 13. Christine M. Nunn and Stephen Neidle. Sequence-Dependent Drug Binding to the Minor Groove of DNA: Crystal Structure of the DNA Dodecamer d(CGCAAATTTGCG)2 Complexed with Propamidine. *J. Med. Chem.* **38**, 2317-2325 (1995).
- 14. George R. Clark, Emily J. Gray, Stephen Neidle, Yu-Hua Li and Werner Leupin. Isohelicity and Phasing in Drug-DNA Sequence Recognition: Crystal Structure of a Tris(benzimidazole)—Oligonucleotide Complex. *Biochemistry* **35**, 13745-13752 (1996).
- 15. Qing Zhang, Tammy J. Dwyer, Vickie Tsui, David A. Case, Junhyeong Cho, Peter B. Dervan and David E. Wemmer. NMR Structure of a Cyclic Polyamide–DNA Complex. *J. Am. Chem. Soc.* **126**, 7958-7966 (2004).
- 16. Guohua Xu, Jiajing Zhao, Na Liu, Minghui Yang, Qiang Zhao, Conggang Li and Maili Liu. Structure-Guided Post-SELEX Optimization of an Ochratoxin A Aptamer. *Nucleic Acids Res.* **47**, 5963-5972 (2019).
- 17. Clara L. Kielkopf, Sarah White, Jason W. Szewczyk, James M. Turner, Eldon E. Baird, Peter B. Dervan and Douglas C. Rees. A Structural Basis for Recognition of A·T and T·A Base Pairs in the Minor Groove of B-DNA. *Science* **282**, 111-115 (1998).
- 18. Clara L. Kielkopf, Eldon E. Baird, Peter B. Dervan and Douglas C. Rees. Structural Basis for G•C Recognition in the DNA Minor Groove. *Nat. Struct. Mol. Biol.* **5**, 104-109 (1998).
- 19. Nadrian C. Seeman. Nucleic Acid Junctions and Lattices. *J. of Theor. Biol.* **99**, 237-247 (1982).
- 20. Nadrian C. Seeman. DNA in a Material World. Nature 421, 427-431 (2003).
- 21. Andre V. Pinheiro, Dongran Han, William M. Shih and Hao Yan. Challenges and Opportunities for Structural DNA Nanotechnology. *Nat. Nanotechnol.* **6**, 763-772 (2011).
- 22. Matthew R. Jones, Nadrian C. Seeman and Chad A. Mirkin. Programmable Materials and the Nature of the DNA Bond. *Science* **347**, 1260901 (2015).
- 23. Nadrian C. Seeman and Hanadi F. Sleiman. DNA Nanotechnology. *Nat. Rev. Mater.* **3**, 17068 (2017).
- 24. Lior Shani, Aaron N. Michelson, Brian Minevich, Yafit Fleger, Michael Stern, Avner Shaulov, Yosef Yeshurun and Oleg Gang. DNA-Assembled Superconducting 3D Nanoscale Architectures. *Nat. Commun.* 11, 5697 (2020).
- 25. Jianping Zheng, Jens J. Birktoft, Yi Chen, Tong Wang, Ruojie Sha, Pamela E. Constantinou, Stephan L. Ginell, Chengde Mao and Nadrian C. Seeman. From Molecular to Macroscopic via the Rational Design of a Self-Assembled 3D DNA Crystal. *Nature* **461**, 74-77 (2009).

- 26. Tao Zhang, Caroline Hartl, Kilian Frank, Amelie Heuer-Jungemann, Stefan Fischer, Philipp C. Nickels, Bert Nickel and Tim Liedl. 3D DNA Origami Crystals. *Adv. Mater.* **30**, 1800273 (2018)
- 27. Paul W. K. Rothemund. Folding DNA to Create Nanoscale Shapes and Patterns. *Nature* **440**, 297-302 (2006).
- 28. Yonggang Ke, Luvena L. Ong, William M. Shih and Peng Yin. Three-Dimensional Structures Self-Assembled from DNA Bricks. *Science* **338**, 1177-1183 (2012).
- 29. Grigory Tikhomirov, Philip Petersen and Lulu Qian. Fractal Assembly of Micrometre-Scale DNA Origami Arrays with Arbitrary Patterns. *Nature* **552**, 67-71 (2017).
- 30. Anna-Katharina Pumm, Wouter Engelen, Enzo Kopperger, Jonas Isensee, Matthias Vogt, Viktorija Kozina, Massimo Kube, Maximilian N. Honemann, Eva Bertosin, Martin Langecker, Ramin Golestanian, Friedrich C. Simmel and Hendrik Dietz. A DNA Origami Rotary Ratchet Motor. *Nature* **607**, 492-498 (2022).
- 31. Karol Woloszyn, Simon Vecchioni, Yoel P. Ohayon, Brandon Lu, Yinglun Ma, Qiuyan Huang, Eric Zhu, Daniel Chernovolenko, Tiffany Markus, Natasa Jonoska, Chengde Mao, Nadrian C. Seeman and Ruojie Sha. Augmented DNA Nanoarchitectures: A Structural Library of 3D Self-Assembling Tensegrity Triangle Variants. *Adv. Mater.*, e2206876 (2022).
- 32. Brandon Lu, Simon Vecchioni, Yoel P. Ohayon, Ruojie Sha, Karol Woloszyn, Bena Yang, Chengde Mao and Nadrian C. Seeman. 3D Hexagonal Arrangement of DNA Tensegrity Triangles. *ACS Nano* **15**, 16788-16793 (2021).
- 33. Chad R. Simmons, Fei Zhang, Jens J. Birktoft, Xiaodong Qi, Dongran Han, Yan Liu, Ruojie Sha, Hatem O. Abdallah, Carina Hernandez, Yoel P. Ohayon, Nadrian C. Seeman and Hao Yan. Construction and Structure Determination of a Three-Dimensional DNA Crystal. *J. Am. Chem. Soc.* **138**, 10047-10054 (2016).
- 34. Chad R. Simmons, Fei Zhang, Tara MacCulloch, Noureddine Fahmi, Nicholas Stephanopoulos, Yan Liu, Nadrian C. Seeman and Hao Yan. Tuning the Cavity Size and Chirality of Self-Assembling 3D DNA Crystals. *J. Am. Chem. Soc.* **139**, 11254-11260 (2017).
- 35. Fei Zhang, Chad R. Simmons, Jade Gates, Yan Liu and Hao Yan. Self-Assembly of a 3D DNA Crystal Structure with Rationally Designed Six-Fold Symmetry. *Angew. Chem. Int. Ed.* 57, 12504-12507 (2018).
- 36. Chad R. Simmons, Tara MacCulloch, Fei Zhang, Yan Liu, Nicholas Stephanopoulos and Hao Yan. A Self-Assembled Rhombohedral DNA Crystal Scaffold with Tunable Cavity Sizes and High-Resolution Structural Detail. *Angew. Chem. Int. Ed.* **59**, 18619-18626 (2020).
- 37. Chad R. Simmons, Tara MacCulloch, Miroslav Krepl, Michael Matthies, Alex Buchberger, Ilyssa Crawford, Jiří Šponer, Petr Šulc, Nicholas Stephanopoulos and Hao Yan. The Influence of Holliday Junction Sequence and Dynamics on DNA Crystal Self-Assembly. *Nat. Commun.* **13**, 3112 (2022).
- 38. Paul J. Paukstelis, Jacek Nowakowski, Jens J. Birktoft and Nadrian C. Seeman. Crystal Structure of a Continuous Three-Dimensional DNA Lattice. *Chem. Biol.* **11**, 1119-1126 (2004).

- 39. Evi Stahl, Florian Praetorius, Carina C. de Oliveira Mann, Karl-Peter Hopfner and Hendrik Dietz. Impact of Heterogeneity and Lattice Bond Strength on DNA Triangle Crystal Growth. *ACS Nano* **10**, 9156-9164 (2016).
- 40. Cosimo Ducani, Corinna Kaul, Martin Moche, William M Shih and Björn Högberg. Enzymatic Production of 'Monoclonal Stoichiometric' Single-Stranded DNA Oligonucleotides. *Nat. Methods* **10**, 647-652 (2013).
- 41. Min Ji, Jiliang Liu, Lizhi Dai, Lei Wang and Ye Tian. Programmable Cocrystallization of DNA Origami Shapes. *J. Am. Chem. Soc.* **142**, 21336-21343 (2020).
- 42. Yasuhide Inokuma, Shota Yoshioka, Junko Ariyoshi, Tatsuhiko Arai, Yuki Hitora, Kentaro Takada, Shigeki Matsunaga, Kari Rissanen and Makoto Fujita. X-Ray Analysis on the Nanogram to Microgram Scale Using Porous Complexes. *Nature* **495**, 461-466 (2013).
- 43. Cheng Tian, Chuan Zhang, Xiang Li, Yingmei Li, Guansong Wang and Chengde Mao. Artificial, Parallel, Left-Handed DNA Helices. *J. Am. Chem. Soc.* **134**, 20273-20275 (2012).
- 44. Brandt F. Eichman, Jeffrey M. Vargason, Blaine H. M. Mooers, and P. Shing Ho. The Holliday junction in an inverted repeat DNA sequence: Sequence effects on the structure of four-way junctions. *Proc. Natl. Acad. Sci. U.S.A.* **97**, 3971-3976 (2000).
- 45. Anastasiya Bavykina, Nikita Kolobov, I Son Khan, Jeremy A. Bau, Adrian Ramirez and Jorge Gascon. Metal-Organic Frameworks in Heterogeneous Catalysis: Recent Progress, New Trends, and Future Perspectives. *Chem. Rev.* **120**, 8468-8535 (2020).
- 46. Song Lin, Christian S. Diercks, Yue-Biao Zhang, Nikolay Kornienko, Eva M. Nichols, Yingbo Zhao, Aubrey R. Paris, Dohyung Kim, Peidong Yang, Omar M. Yaghi and Christopher J. Chang. Covalent Organic Frameworks Comprising Cobalt Porphyrins for Catalytic CO(2) Reduction in Water. *Science* **349**, 1208-1213 (2015).
- 47. Zhe Li, Longfei Liu, Mengxi Zheng, Jiemin Zhao, Nadrian C. Seeman and Chengde Mao. Making Engineered 3D DNA Crystals Robust. *J. Am. Chem. Soc.* **141**, 15850-15855 (2019).
- 48. Jian-Rong Li, Julian Sculley and Hong-Cai Zhou. Metal-Organic Frameworks for Separations. *Chem. Rev.* **112**, 869-932 (2012).
- 49. Eric D. Bloch, Wendy L. Queen, Rajamani Krishna, Joseph M. Zadrozny, Craig M. Brown and Jeffery R. Long. Hydrocarbon Separations in a Metal-Organic Framework with Open Iron(II) Coordination Sites. *Science* **335**, 1606-1610 (2012).
- 50. Kaushik Dey, Manas Pal, Kanhu C. Rout, Shebeeb Kunjattu, Anuja Das, Rabibrata Mukherjee, Ulhas K. Kharul and Rahul Banerjee. Selective Molecular Separation by Interfacially Crystallized Covalent Organic Framework Thin Films. *J. Am. Chem. Soc.* **139**, 13083-13091 (2017).
- 51. Paul J. Paukstelis. Three-Dimensional DNA Crystals as Molecular Sieves. *J. Am. Chem. Soc.* **128**, 6794-6795 (2006).
- 52. Lulu Qian and Erik Winfree. Scalilng up digital circuit computation with DNA strand displacement cascades. *Science* **332**, 1196-1201 (2011).

- 53. Lulu Qian, Erik Winfree and Jehoshua Bruck. Neural network computation with DNA strand displacement cascades. *Nature* **475**, 368-372 (2011).
- 54. Luis Ceze, Jeff Nivala and Karin Strauss. Molecular digital data storage using DNA. *Nat. Rev. Genet.* **20**, 456-466 (2019).
- 55. Mengxi Zheng, Zhe Li, Cuizheng Zhang, Nadrian C. Seeman and Chengde Mao. Powering Approximately 50 Microm Motion by a Molecular Event in DNA Crystals. *Adv. Mater.* **34**, e2200441 (2022).
- 56. Mohamed Eddaoudi, Jaheon Kim, Nathaniel Rosi, David Vodak, Joseph Wachter, Michael O'Keeffe and Omar M. Yaghi. Systematic Design of Pore Size and Functionality in Isoreticular MOFs and their Application in Methane Storage. *Science* **295**, 469-472 (2002).

TOC graphic

